

Accessing structure of protons and nuclei at small x at the Electron-Ion Collider

Wenbin Zhao

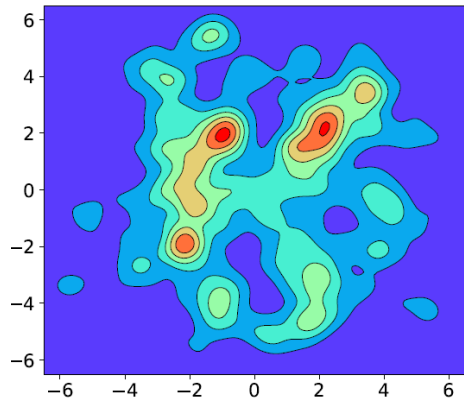
Wayne State University, Brookhaven National Laboratory

Collaborators: Heikki Mäntysaari, Björn Schenke, and Chun Shen

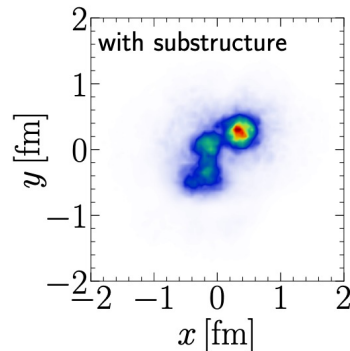
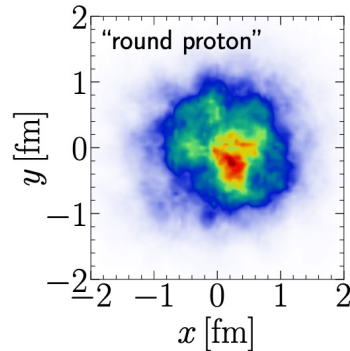
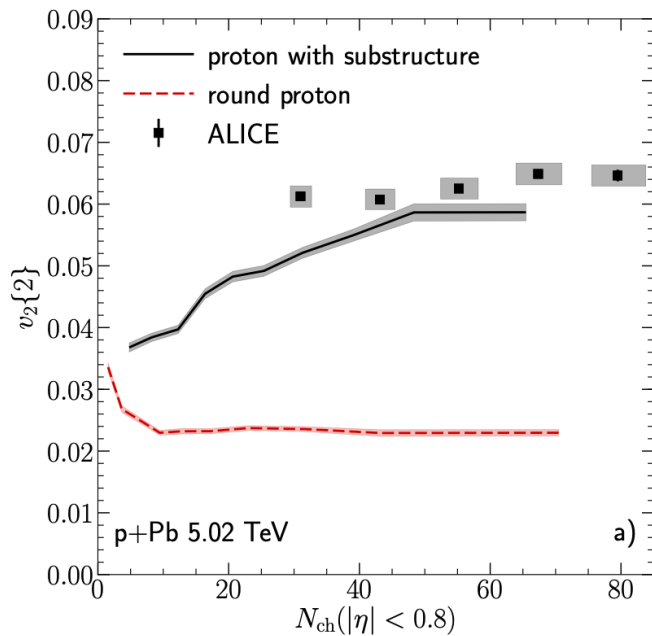
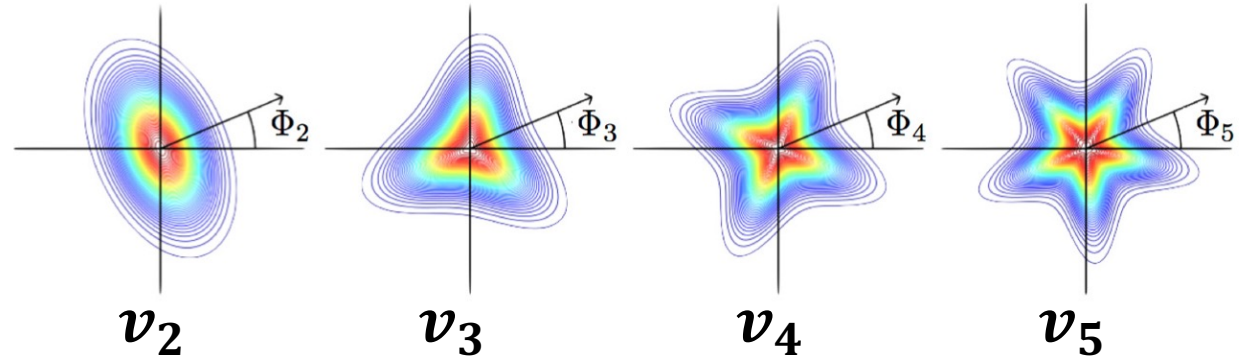
Apr. 14, 2023, GHP2023



Hydrodynamics response to collision geometry



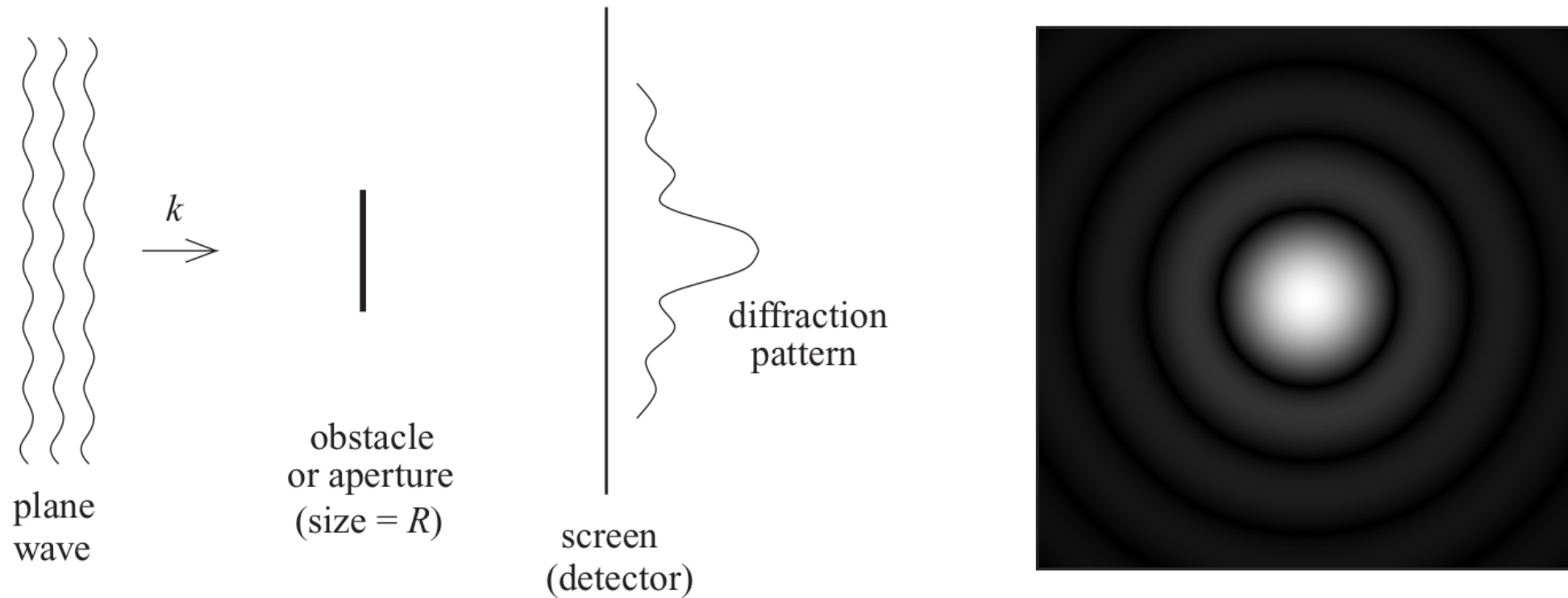
Hydrodynamics



- Heavy-ion Collisions: Initial spatial geometry \Rightarrow final momentum anisotropy.
- Proton's sub-nucleonic structure is crucial to understand the collectivity in small collision systems

B. Schenke, Rept. Prog. Phys. 84, 082301 (2021).

Constrain fluctuating proton geometry from DIS

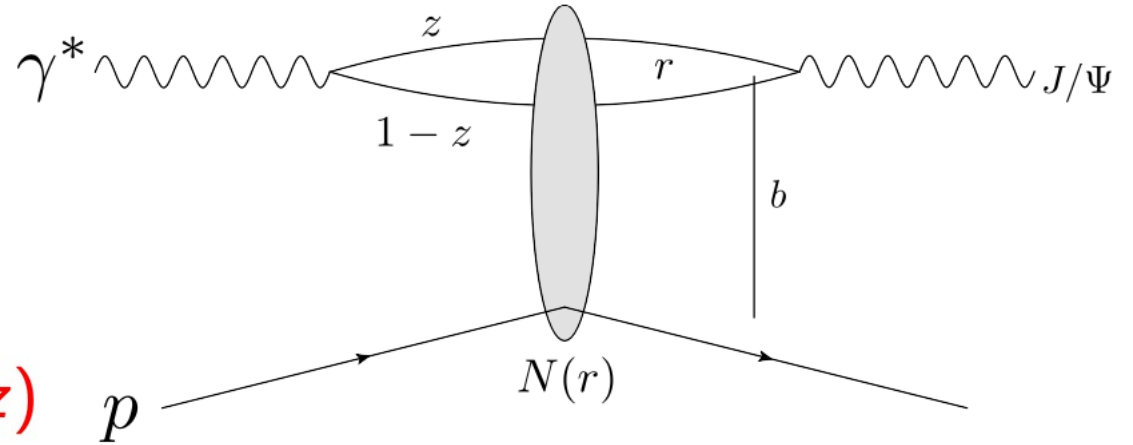


Yuri V. Kovchegov, QUANTUM CHROMODYNAMICS AT HIGH ENERGY. Wiki.

Diffractive vector meson production

High energy factorization:

- 1 $\gamma^* \rightarrow q\bar{q}$ splitting, wave function $\Psi^\gamma(r, Q^2, z)$
- 2 $q\bar{q}$ dipole scatters elastically
- 3 $q\bar{q} \rightarrow J/\psi$, wave function $\Psi^V(r, Q^2, z)$



Diffractive scattering amplitude

Theoretically: no net color transfer

$$\mathcal{A}^{\gamma^* p \rightarrow V p} \sim \int d^2 b dz d^2 r \Psi^{\gamma^*} \Psi^V(r, z, Q^2) e^{-i\mathbf{b} \cdot \mathbf{\Delta}} N(r, x, b)$$

Impact parameter, b , is the Fourier conjugate of the momentum transfer, $\Delta \approx \sqrt{-t}$

$N(\mathbf{r}_T, \mathbf{b}_T, x) = 1 - \exp(-\mathbf{r}_T^2 F(\mathbf{r}_T, x) T_p(\mathbf{b}_T))$ accesses to the spatial structure ($T_{p/A}$)

$F(\mathbf{r}_T, x) = \frac{\pi^2}{2N_c} \alpha_s(\mu^2) x g(x, \mu^2)$. $xg(x, \mu^2)$, gluon density at x and scale μ^2 ($\mu^2 \sim \mu_0^2 + 1/r_T^2$).

Miettinen, Pumplin, PRD 18, 1978; Caldwell, Kowalski, 0909.1254; Mäntysaari, Schenke, 1603.04349; Mäntysaari, 2001.10705

Coherent and incoherent processes

- **Coherent**

$$\sigma_{\text{coherent}} \sim |\langle \mathcal{A} \rangle_{\Omega}|^2$$

Target stays intact, ($\langle \text{initial state} | = | \text{final state} \rangle$)
Probes the average shape of the target.

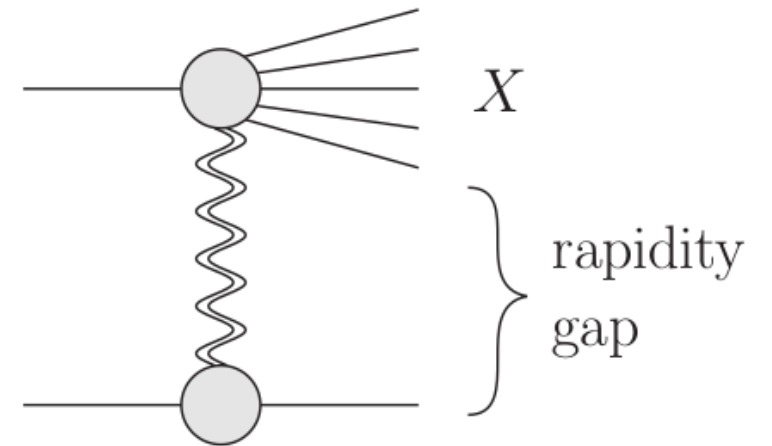
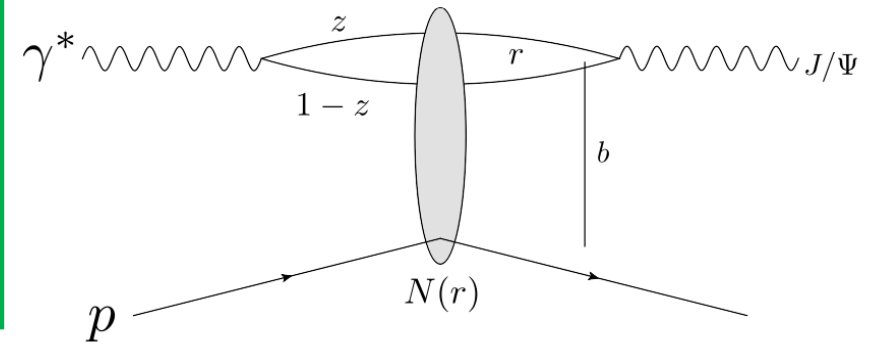
- **Incoherent**

$$\sigma_{\text{incoherent}} \sim \langle |\mathcal{A}|^2 \rangle_{\Omega} - |\langle \mathcal{A} \rangle_{\Omega}|^2$$

Target breaks apart, ($\langle \text{initial state} | \neq | \text{final state} \rangle$)
Probes the variance of event-by-event initial state fluctuations in target structure.

- Experimental signature: rapidity gap.
- Theoretically: no net color transfer.

Miettinen, Pumplin, PRD 18, 1978; Caldwell, Kowalski, 0909.1254; Mäntysaari, Schenke, 1603.04349; Mäntysaari, 2001.10705



Proton geometry fluctuations

- Proton's event-by-event fluctuating density profile:

$$T_p(\mathbf{b}_\perp) = \frac{1}{N_q} \sum_{i=1}^{N_q} p_i T_q(\mathbf{b}_\perp - \mathbf{b}_{\perp,i}), \quad P(\ln p_i) = \frac{1}{\sqrt{2\pi\sigma}} \exp\left[-\frac{\ln^2 p_i}{2\sigma^2}\right].$$

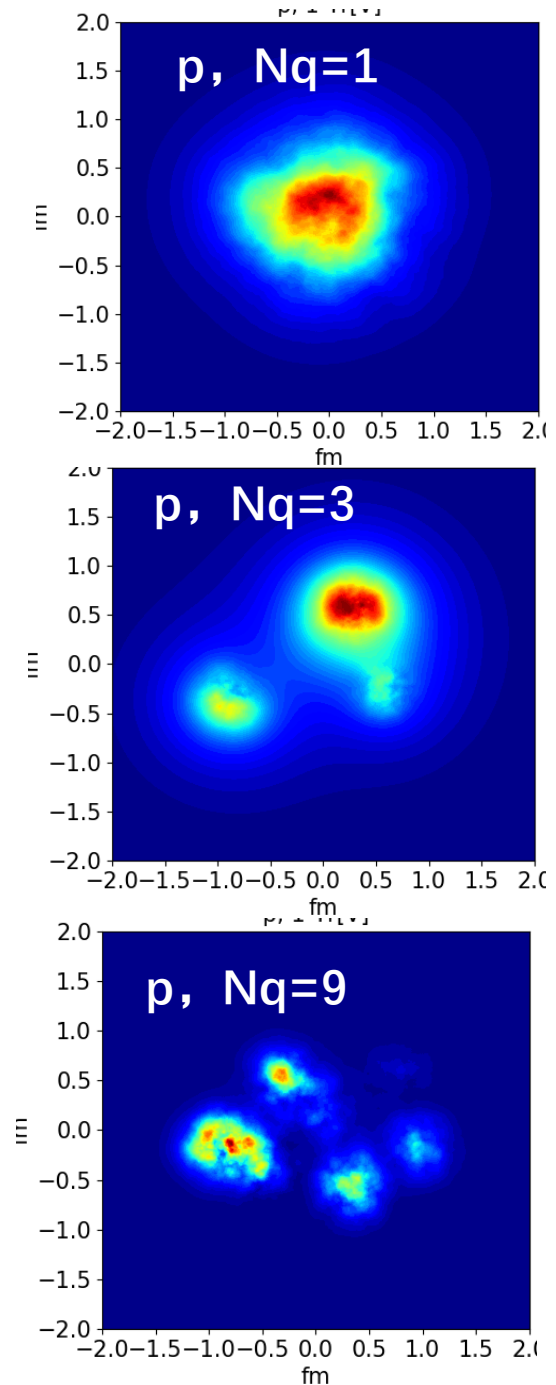
- The density profile of each spot is:

$$T_q(\vec{b}) = \frac{1}{2\pi B_q} e^{-b^2/(2B_q)}$$

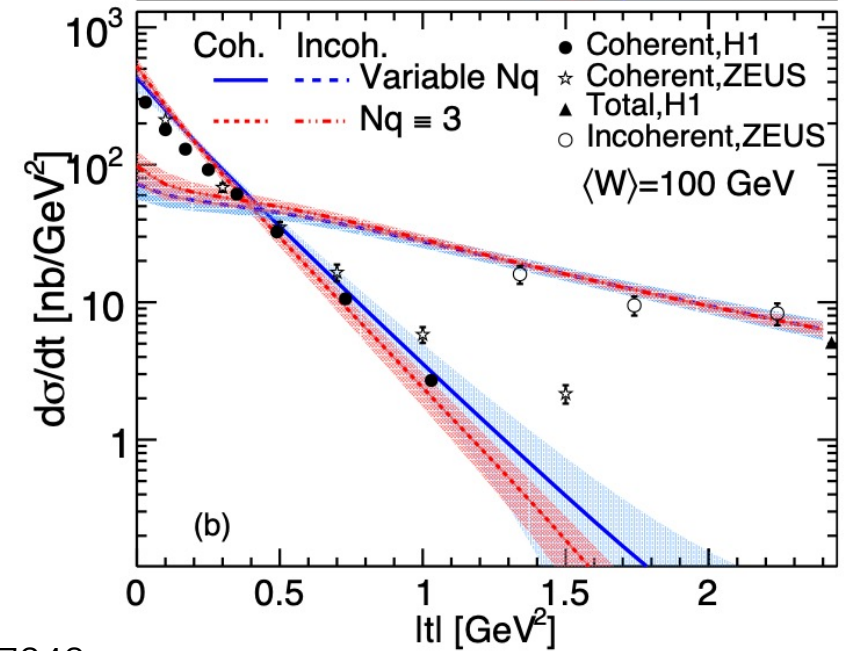
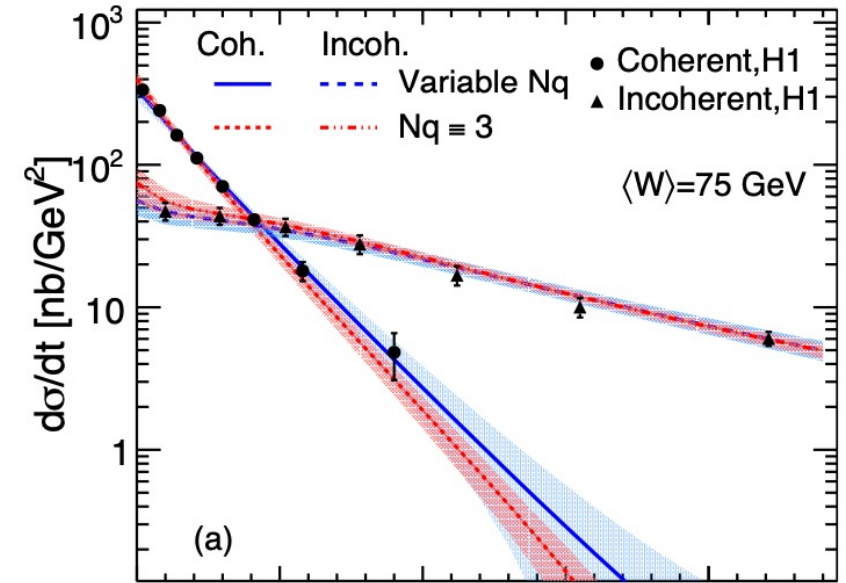
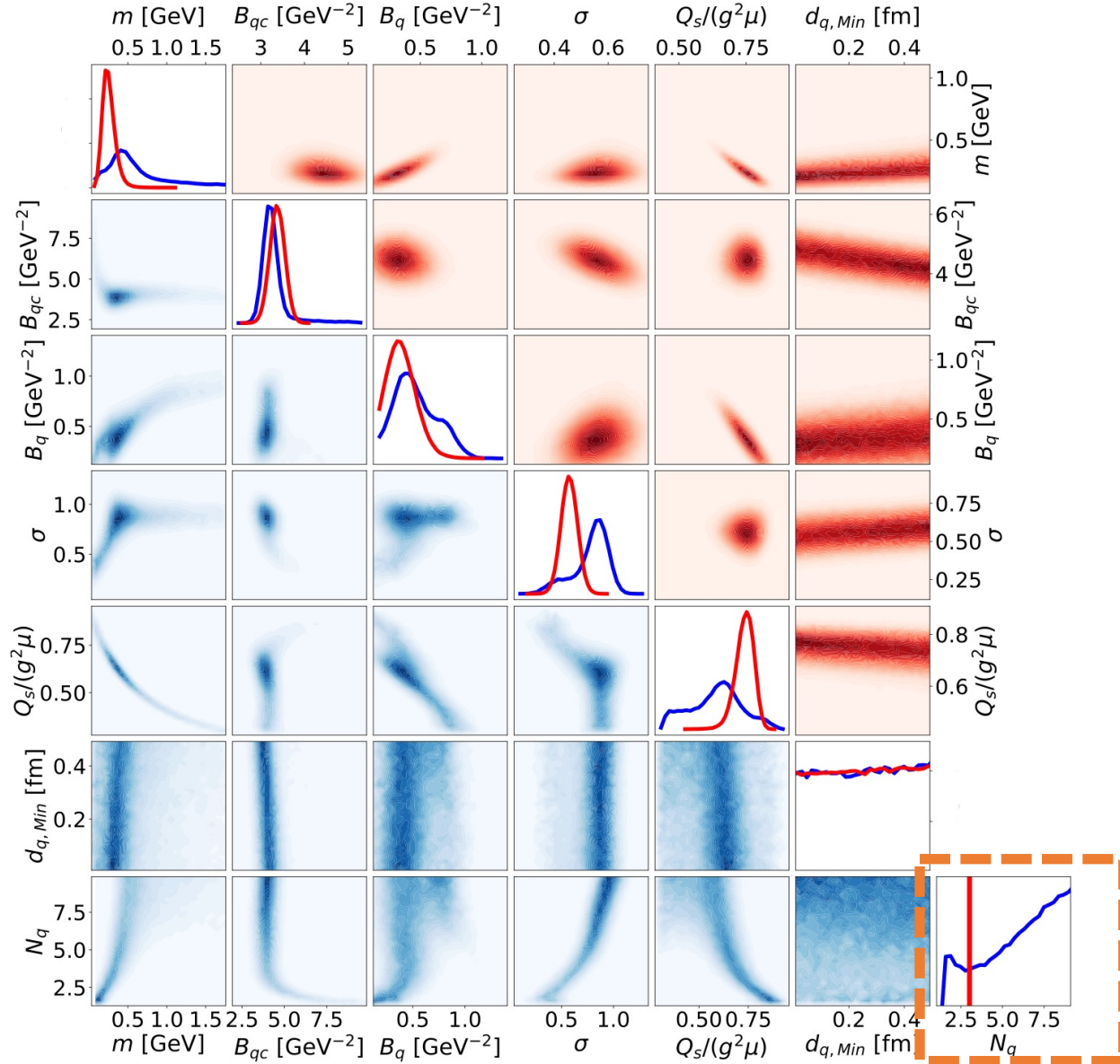
- The spot positions \vec{b}_i are sampled from:

$$P(b_i) = \frac{1}{2\pi B_{qc}} e^{-b_i^2/(2B_{qc})}$$

Schenke , etc.al. PhysRevLett.108.252301 ,
 PhysRevC.86.034908, Mäntysaari, Schenke, 1603.04349;

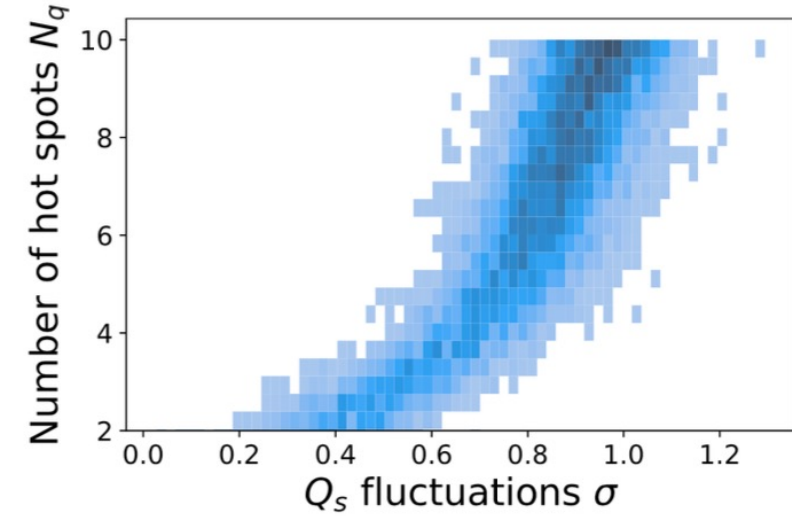
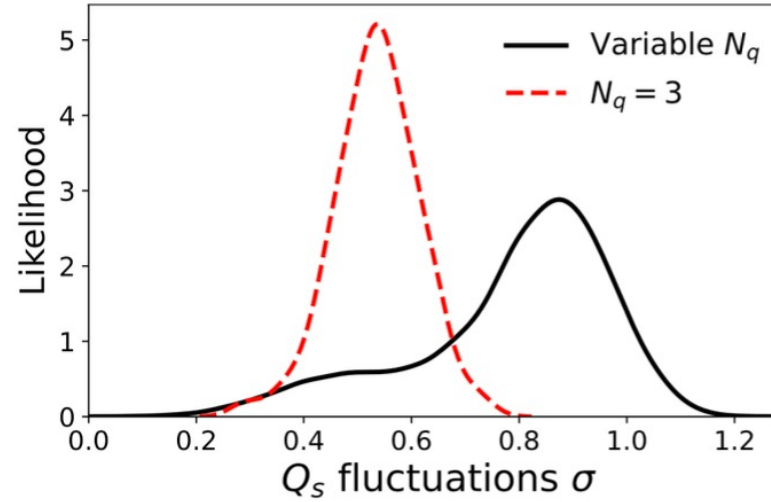
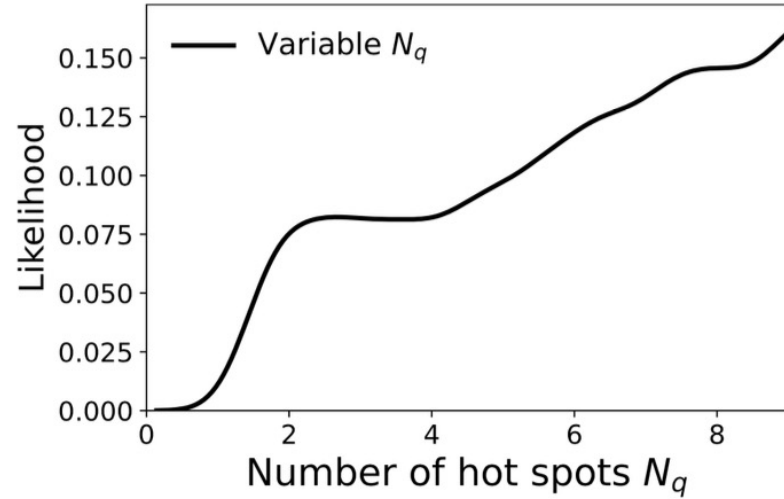


Posterior Distribution



H.Mantysaari, B.Schenke, C. Shen and W. Zhao, Phys. Lett. B 833 (2022), 137348.

Degeneracy in the number of hot spots



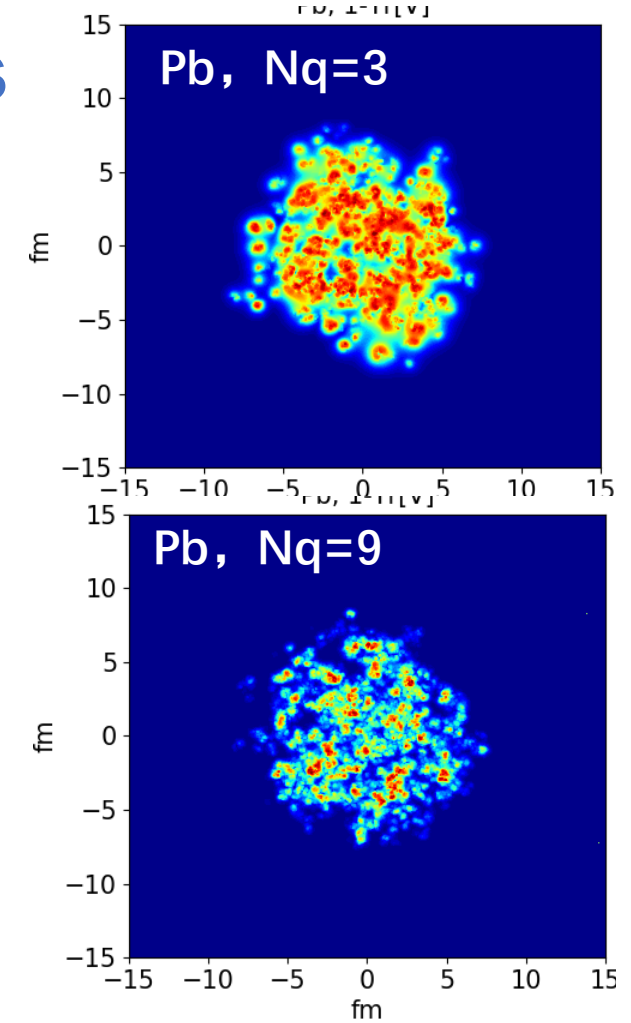
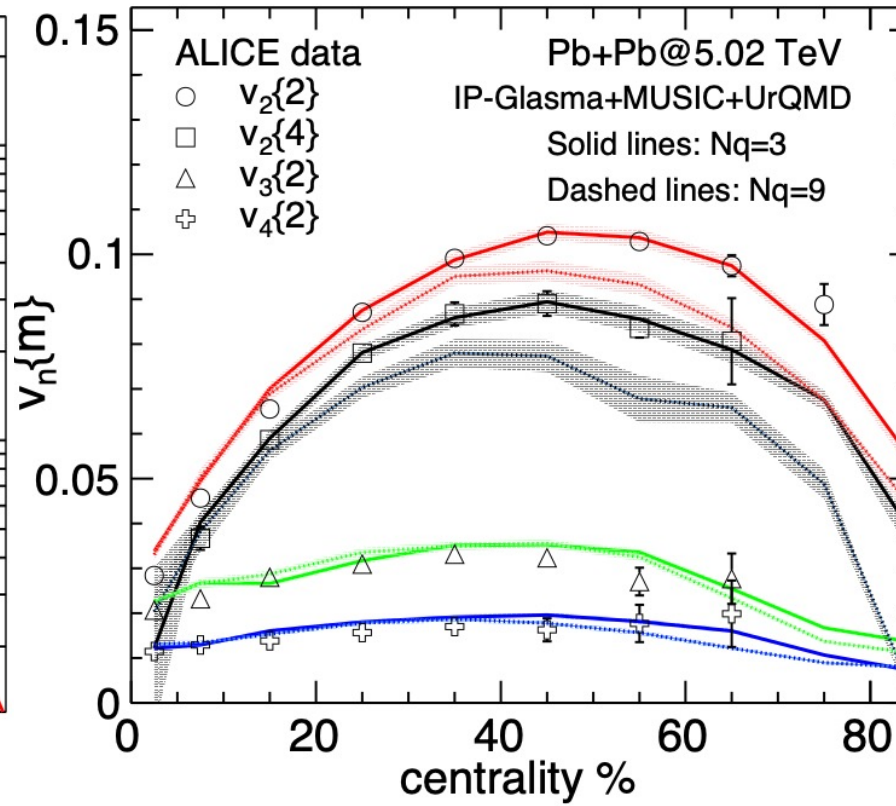
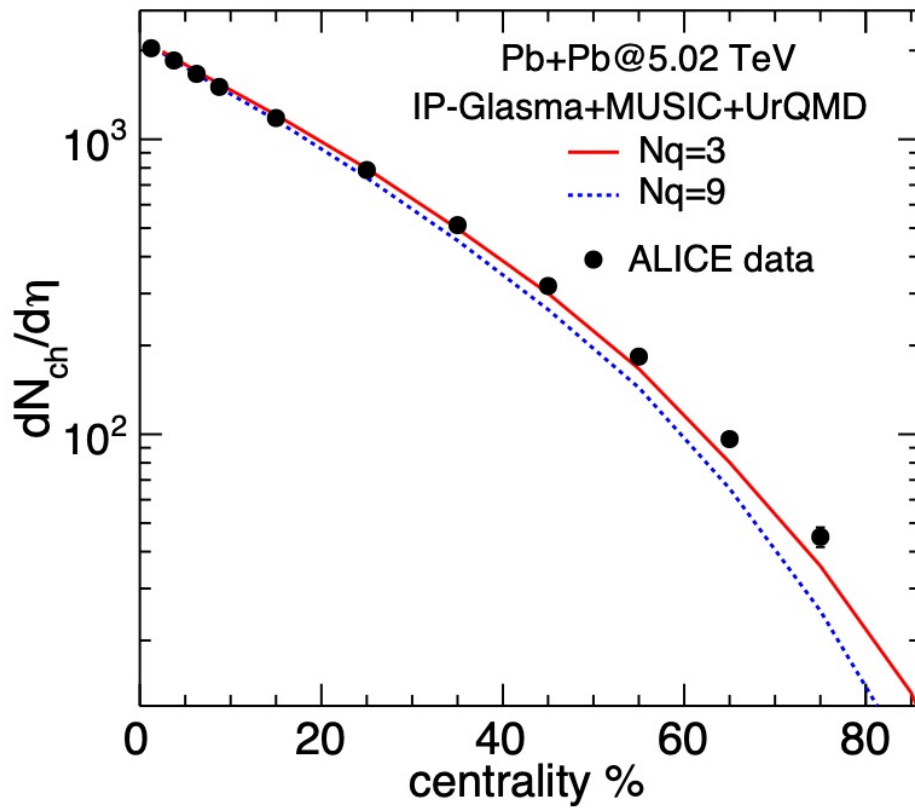
- The likelihood of number of hot spots N_q increases monotonously.
- Large N_q partially compensated by large Q_s fluctuations, $\sigma \propto \sqrt{N_q}$, “number of effective hot spots” $< N_q$
- Proton’s event-by-event fluctuating density profile:

$$T_p(\mathbf{b}_\perp) = \frac{1}{N_q} \sum_{i=1}^{N_q} p_i T_q(\mathbf{b}_\perp - \mathbf{b}_{\perp,i}), \quad P(\ln p_i) = \frac{1}{\sqrt{2\pi}\sigma} \exp\left[-\frac{\ln^2 p_i}{2\sigma^2}\right].$$

H. Mantysaari, B.Schenke, C. Shen and W. Zhao, Phys. Lett. B 833 (2022), 137348.

H. Mantysaari, B.Schenke, C. Shen and W. Zhao, [arXiv:2208.00396 [hep-ph]].

Connecting to Relativistic Nuclear Collisions

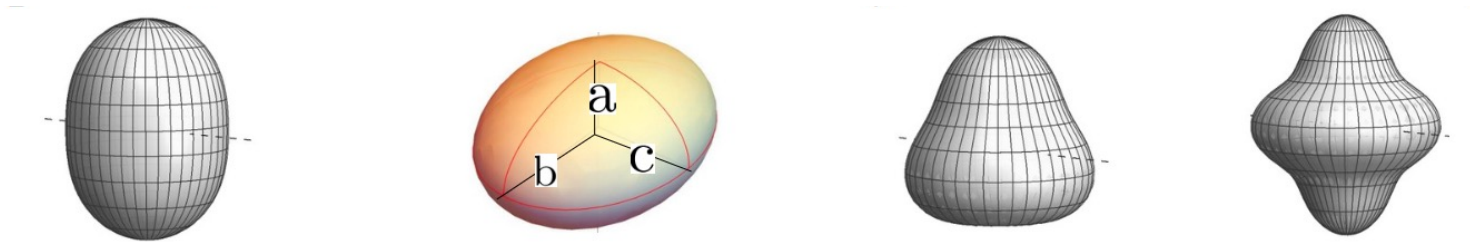


- The multiplicity distributions and elliptic flow coefficients in Pb+Pb collisions favor the small Nq case.

H.Mantysaari, B.Schenke, C. Shen and W. Zhao, Phys. Lett. B 833 (2022), 137348.

H.Mantysaari, B.Schenke, C. Shen and W. Zhao, [arXiv:2208.00396 [hep-ph]].

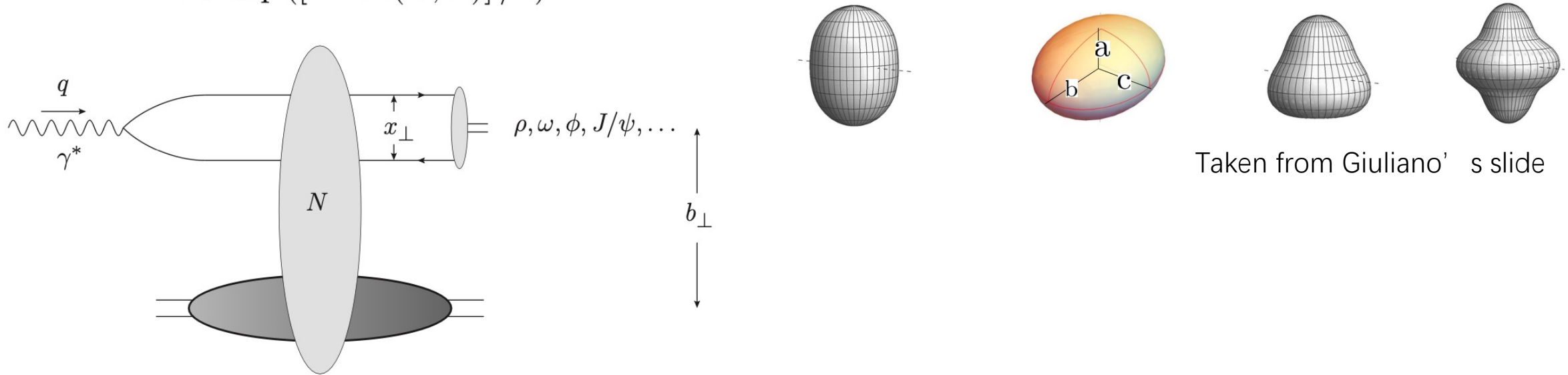
Accessing nuclear deformation at small x



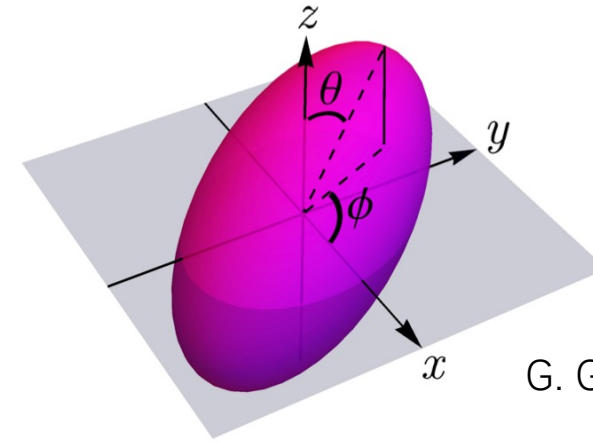
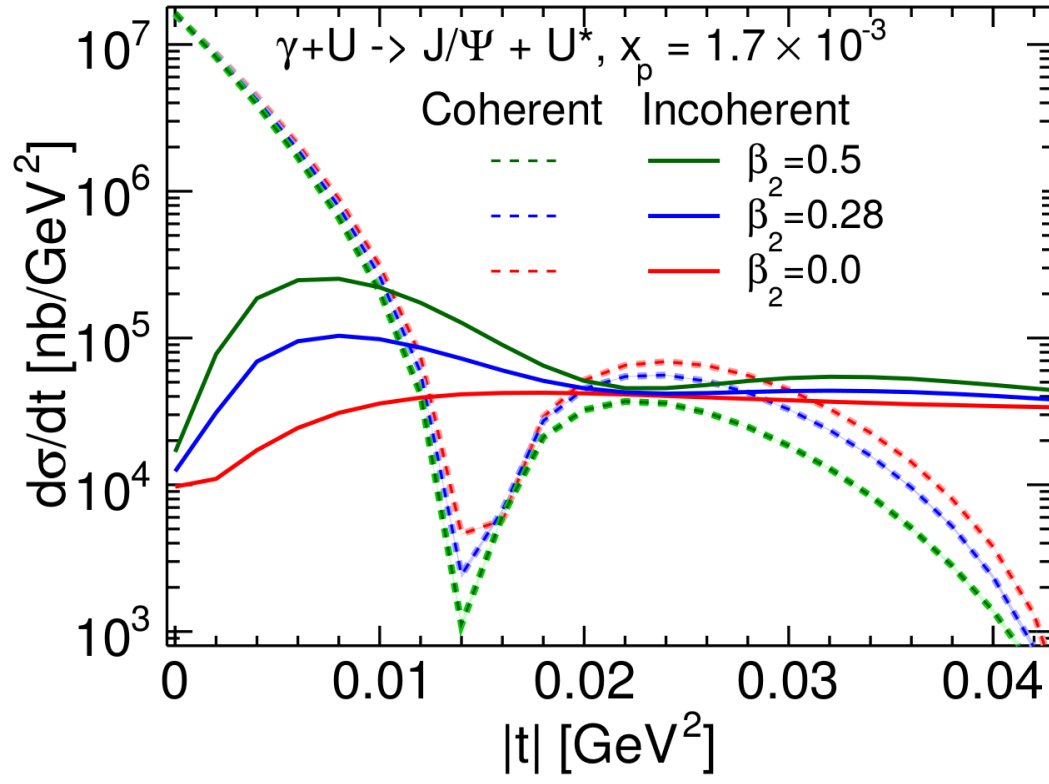
Nuclear structure

Generalized Woods-Saxon profile

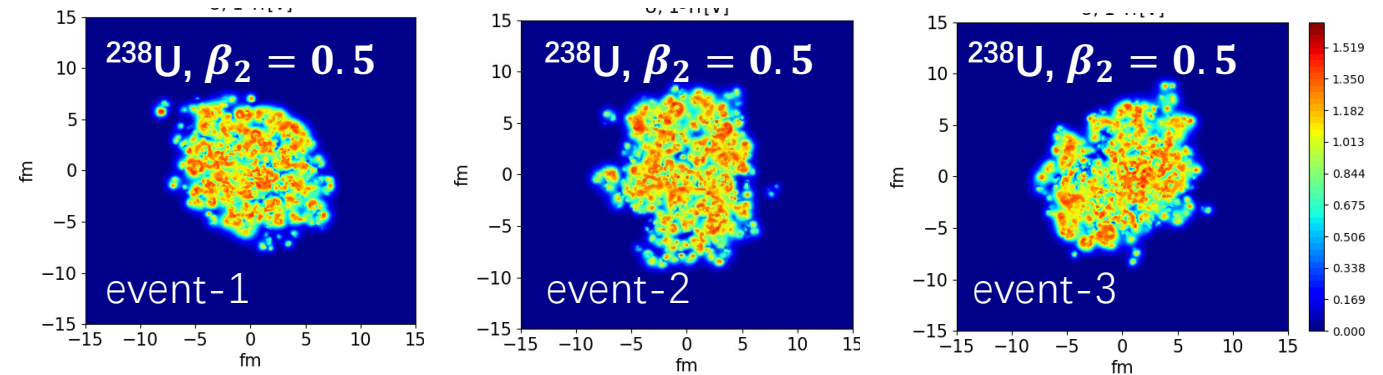
$$\rho(r, \Theta, \Phi) \propto \frac{1}{1 + \exp([r - R(\Theta, \Phi)]/a)}, \quad R(\Theta, \Phi) = R_0 \left[1 + \underline{\beta_2} \left(\cos \gamma Y_{20}(\Theta) + \sin \gamma \underline{Y_{22}}(\Theta, \Phi) \right) + \underline{\beta_3} Y_{30}(\Theta) + \underline{\beta_4} Y_{40}(\Theta) \right]$$



- Sample nucleon positions based on the Wood—Saxon distribution.
- Different deformation parameters controls the geometric deformation at different length scale.
- Probe the nuclear geometric deformation (deformed gluon density distributions) by the diffractive process.



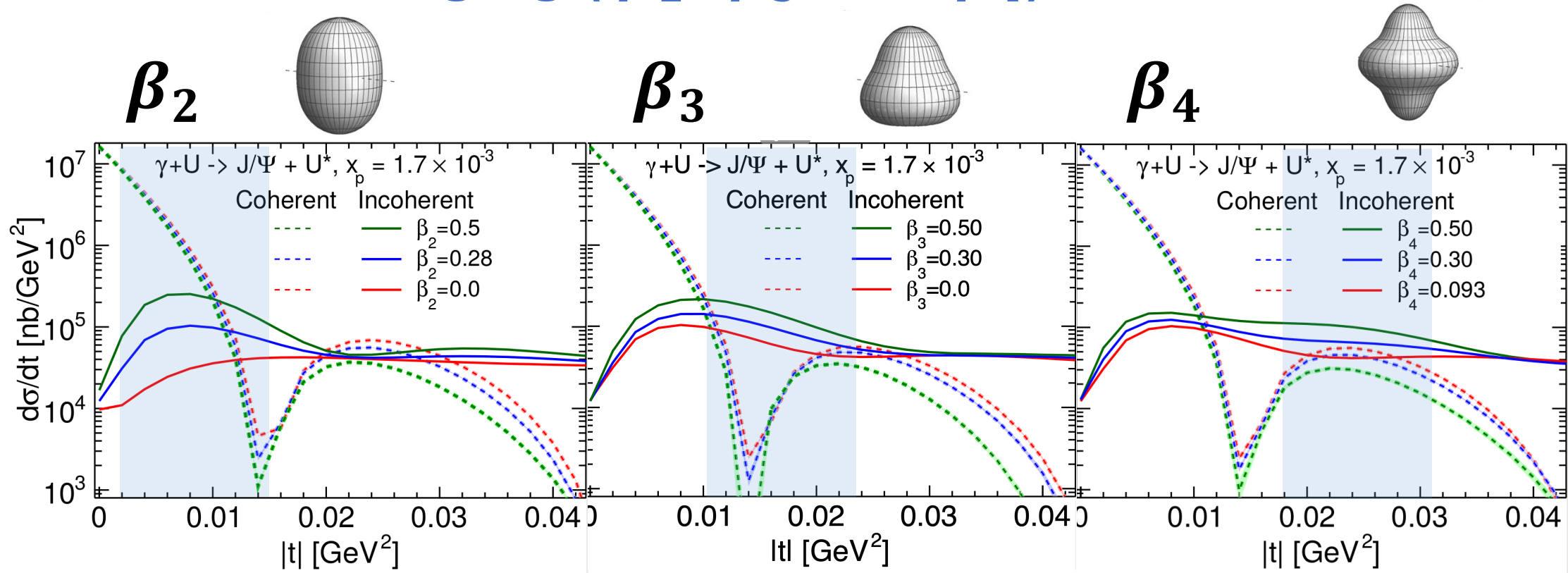
G. Giacalone, arXiv: 2004.14463



- With $\beta > 0$, the configurations projected onto x-y plane have great fluctuations.
- β_2 quadrupole deformation of the nucleus affects incoherent cross section at small $|t|$ (large length scales) and provides direct information on the nuclear structure at small x .

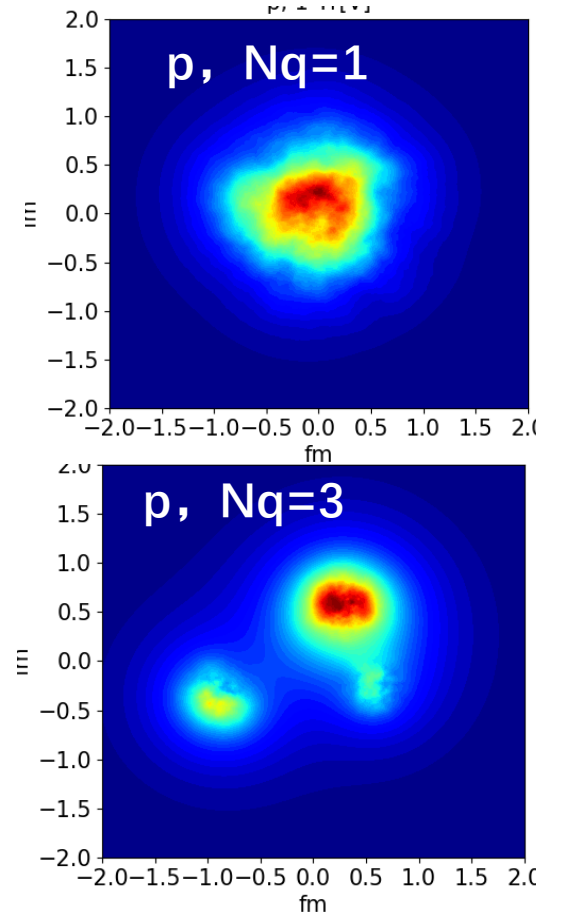
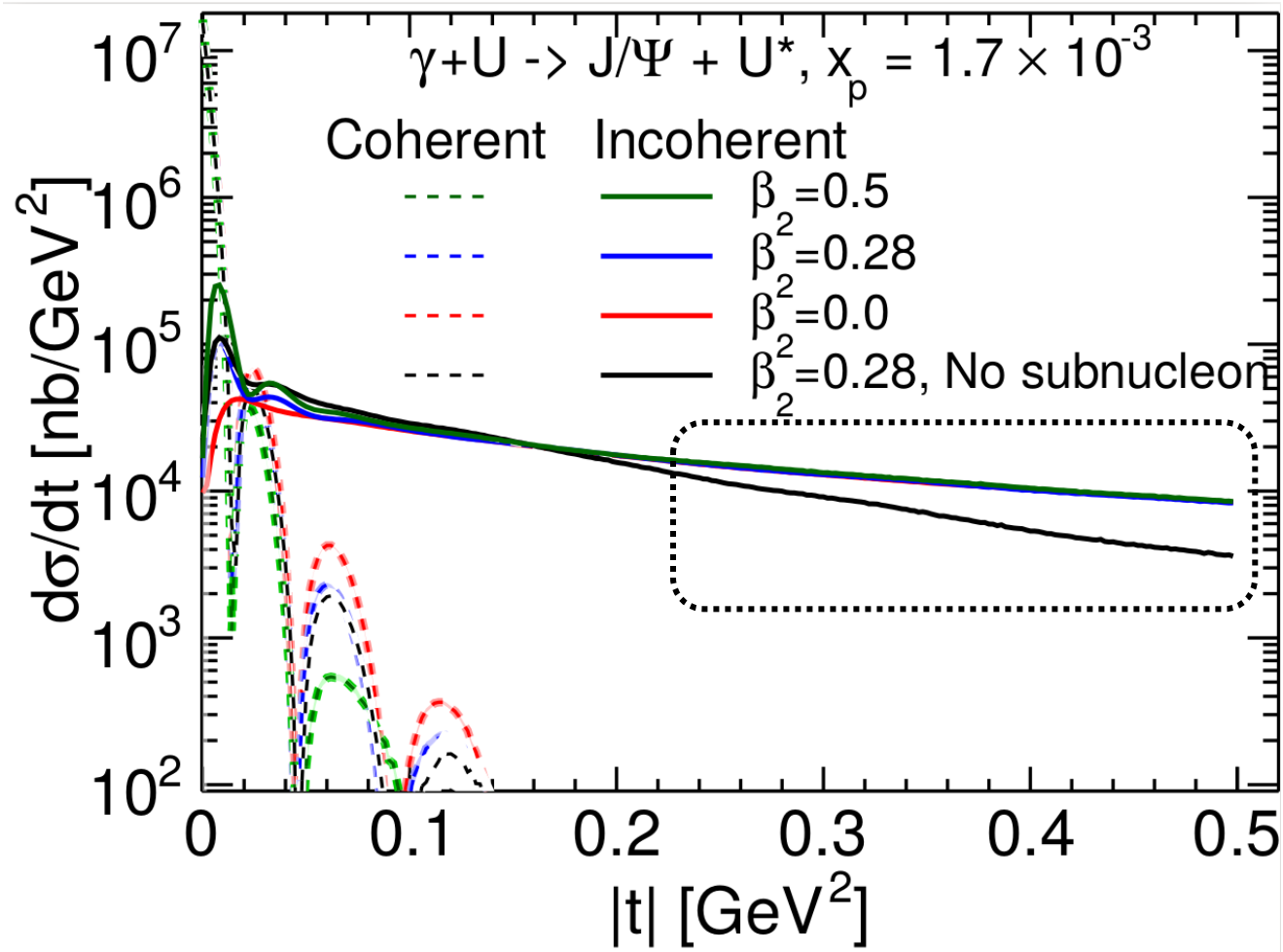
H.Mantysaari, B.Schenke, C. Shen and W. Zhao, [arXiv:2303.04866].

Multi-scale imaging (β_2 , β_3 , and β_4)



- β_2 , β_3 and β_4 manifest themselves at different $|t|$ regions (different length scales).

"See" sub-nucleon structures

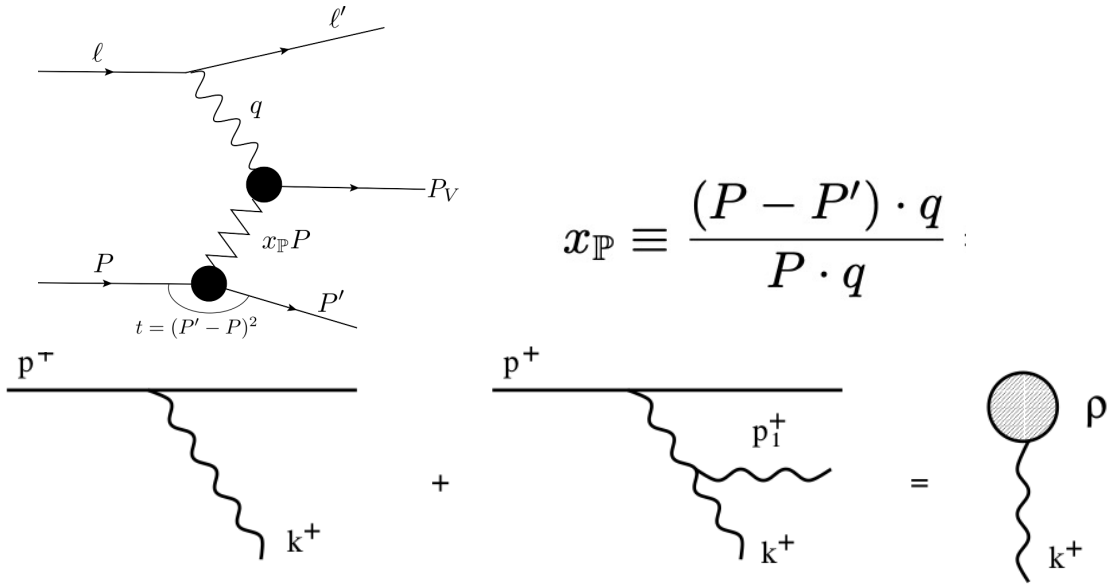


- High $|t|$ region of $\gamma^* + A$ incoherent cross section probes sub-nucleon structures.

H.Mantysaari, B.Schenke, C. Shen and W. Zhao, Phys. Lett. B 833 (2022), 137348.

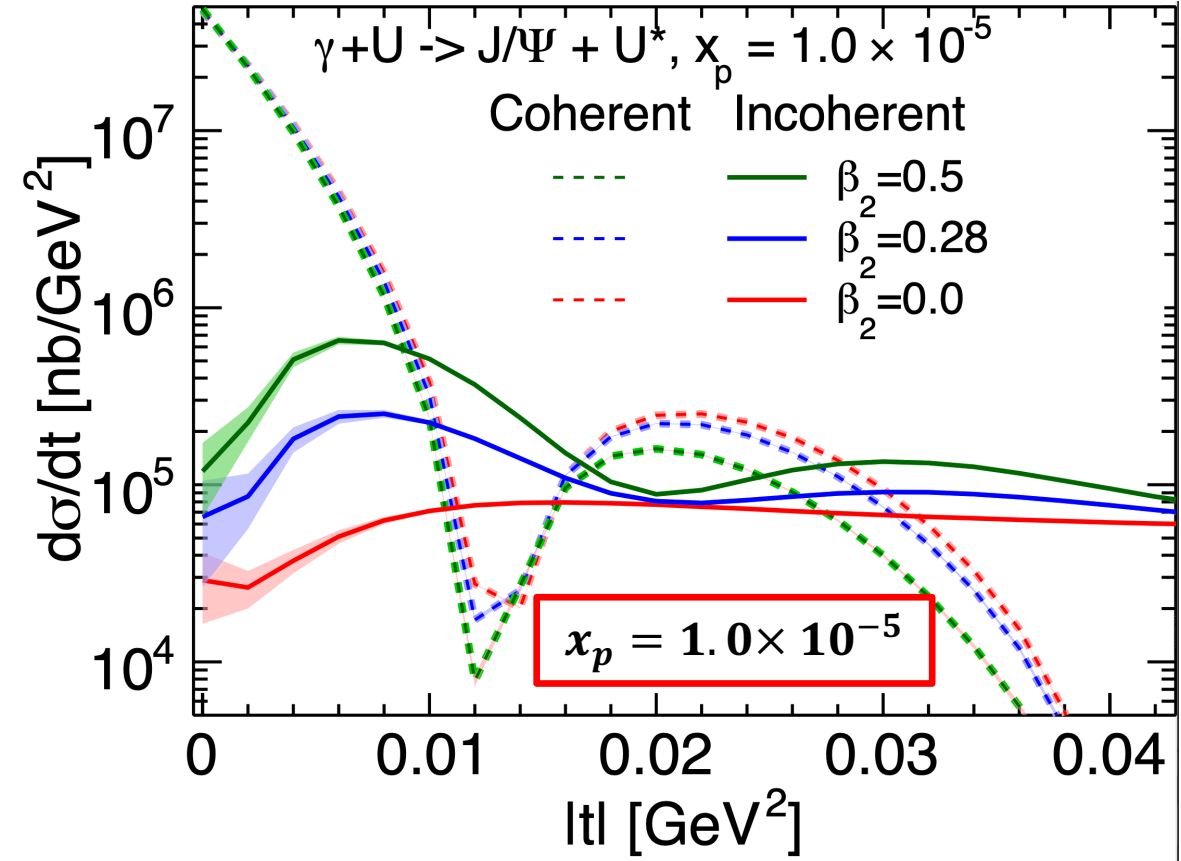
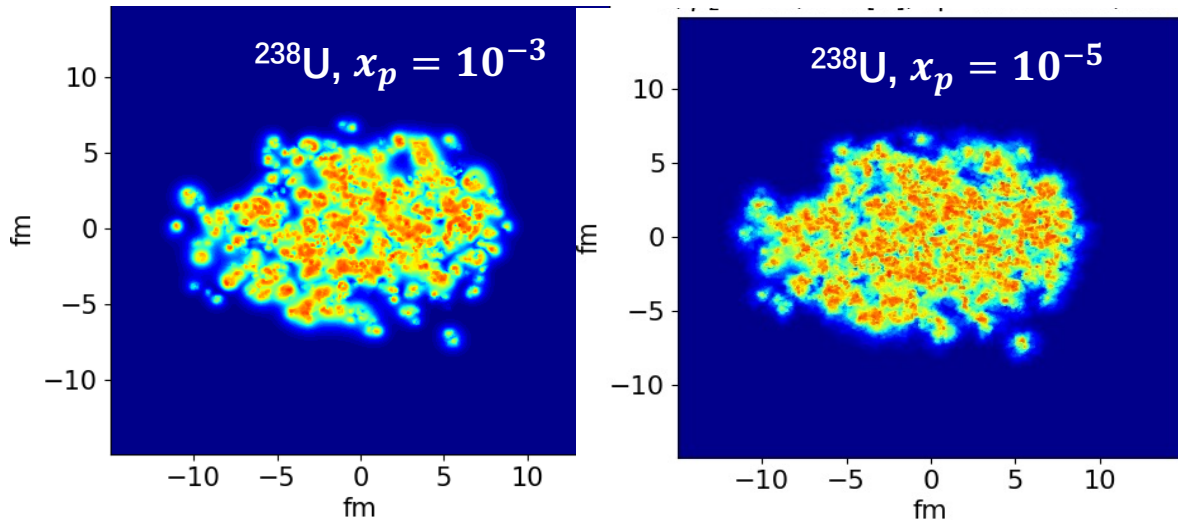
H.Mantysaari, B.Schenke, C. Shen and W. Zhao, [arXiv:2303.04866].

JIMWLK evolution to smaller xp



$$x_P \equiv \frac{(P - P') \cdot q}{P \cdot q}$$

- JIMWLK: absorb quantum fluctuations at intermediate x range as the color sources of smaller x .



- JIMWLK evolution doesn't wash out this effects.

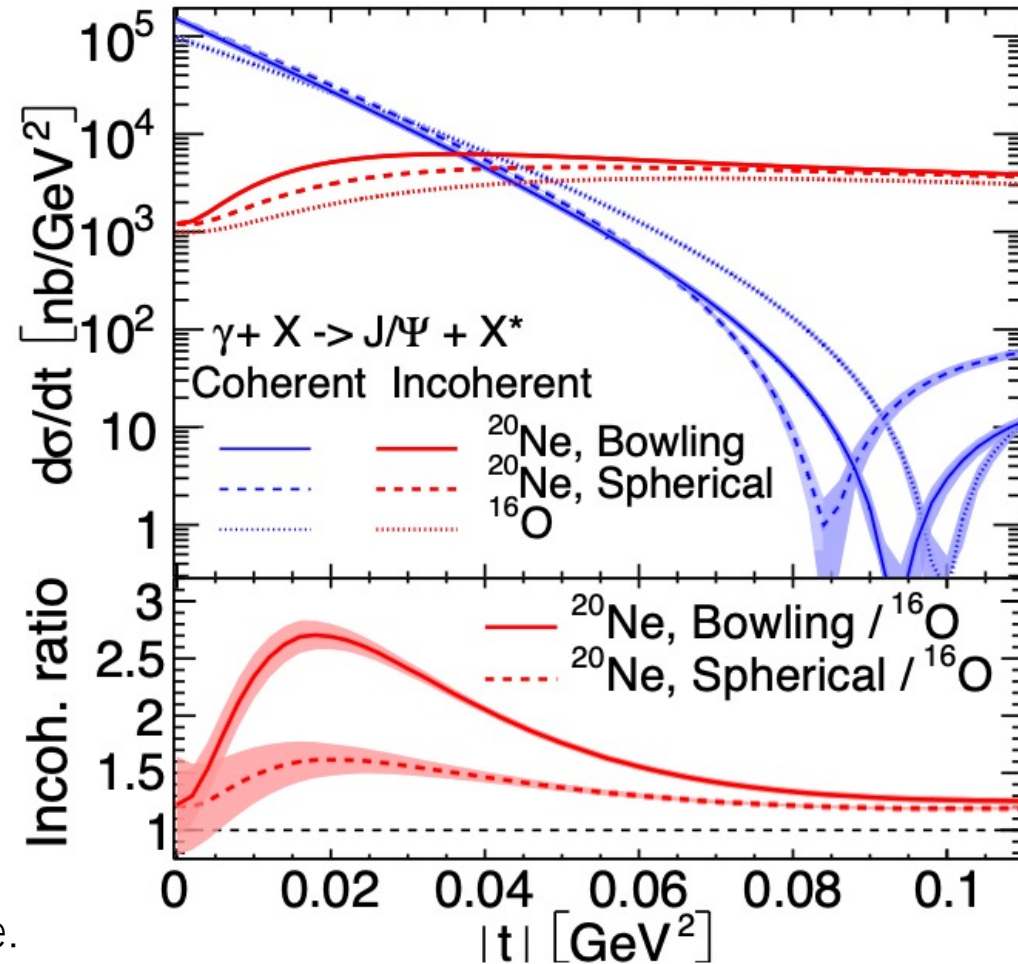
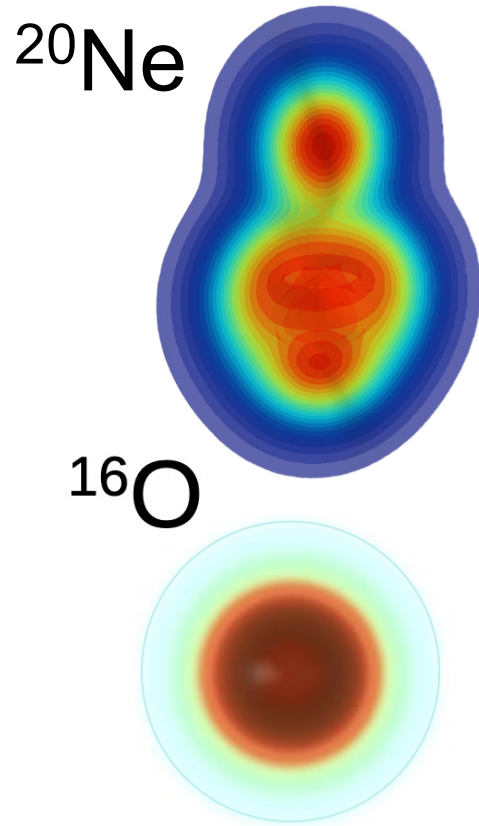
H.Mantysaari, B.Schenke, C. Shen and W. Zhao, [arXiv:2303.04866].

H.Mantysaari, B.Schenke PRD, 98, 034013.

T. Lappi and H. Mantysaari, EPJC 73, 2307 (2013).

Yuri V. Kovchegov, QUANTUM CHROMODYNAMICS AT HIGH ENERGY

Probing ^{20}Ne and ^{16}O



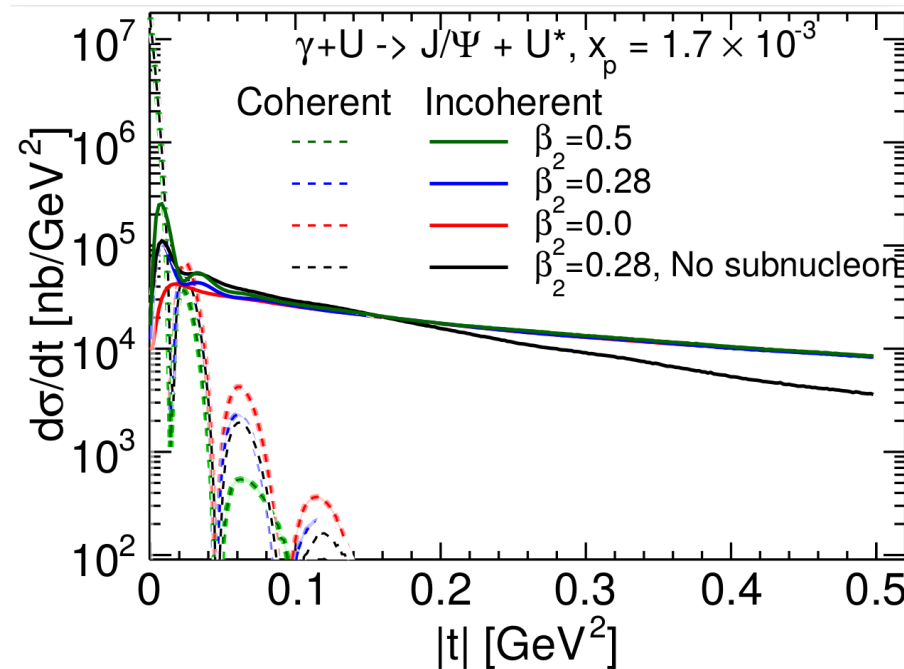
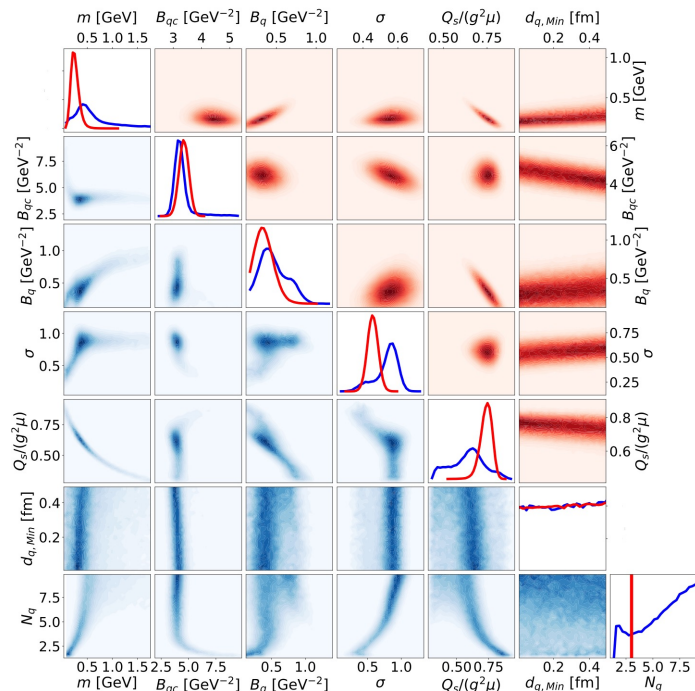
Nucleon density distribution is taken from G. Giacalone.

- Incoherent cross section at small $|t|$ captures the deformation of the ^{20}Ne .
- Significant difference between ^{20}Ne and ^{16}O diffractive cross sections is observed.

H.Mantysaari, B.Schenke, C. Shen and W. Zhao, [arXiv:2303.04866].

Summary

- We perform the first Bayesian analysis to constrain the proton shape fluctuations from diffractive J/Ψ data at HERA.
- Diffractive vector meson production can “see” the nuclear shape and fluctuations at different scales!
- JIMWLK evolution doesn’t wash out this effect.



Thanks for Your Attentions!

I acknowledge financial support from The Gordon and Betty Moore Foundation and the American Physical Society to present this work at the GHP 2023 workshop!

Back Up

Back Up